Bulletin of the Seismological Society of America, 90, 1, pp. 1–21, February 2000

A Time-Dependent Probabilistic Seismic-Hazard Model for California

by Chris H. Cramer,* Mark D. Petersen,† Tianqing Cao,
Tousson R. Toppozada, and Michael Reichle

Abstract For the purpose of sensitivity testing and illuminating nonconsensus components of time-dependent models, the California Department of Conservation, Division of Mines and Geology (CDMG) has assembled a time-dependent version of its statewide probabilistic seismic hazard (PSH) model for California. The model incorporates available consensus information from within the earth-science community, except for a few faults or fault segments where consensus information is not available. For these latter faults, published information has been incorporated into the model. As in the 1996 CDMG/U.S. Geological Survey (USGS) model, the time-dependent models incorporate three multisegment ruptures: a 1906, an 1857, and a southern San Andreas earthquake. Sensitivity tests are presented to show the effect on hazard and expected damage estimates of (1) intrinsic (aleatory) sigma, (2) multisegment (cascade) vs. independent segment (no cascade) ruptures, and (3) time-dependence vs. time-independence. Results indicate that (1) differences in hazard and expected damage estimates between time-dependent and independent models increase with decreasing intrinsic sigma, (2) differences in hazard and expected damage estimates between full cascading and not cascading are insensitive to intrinsic sigma, (3) differences in hazard increase with increasing return period (decreasing probability of occurrence), and (4) differences in moment-rate budgets increase with decreasing intrinsic sigma and with the degree of cascading, but are within the expected uncertainty in PSH time-dependent modeling and do not always significantly affect hazard and expected damage estimates.

Introduction

A time-dependent probabilistic seismic-hazard (PSH) model is felt by some to be important in loss assessments for insurance and risk management. In time-dependent models, the probability of earthquake occurrence increases with the elapsed time since the last large or characteristic earthquake on a fault or fault segment. A characteristic earthquake for a fault is an earthquake that essentially ruptures the entire area of the fault or fault segment. A time-dependent model for a given fault is characterized by its recurrence-interval probability-density function (distribution of times between large earthquakes), which often has a fixed coefficient of variation (standard deviation divided by the mean). This coefficient of variation (cov) can be used to indicate whether a time-dependent model is quasiperiodic (cov < 1) or clustered (cov > 1) (Wu *et al.,* 1995). For some faults, there is not enough information for time-dependent modeling. We have modeled these faults using Poisson or time-independent PSH models. In a Poisson model, the probability remains constant for any time period and has cov $=$ 1, by definition.

For most faults, we do not have adequate information to constrain time-dependent probabilities. However, for a few faults for which we think we have adequate information on time-dependent behavior, a time-dependent PSH model may be better at identifying the short-term risks for economic loss assessment. In California, time-dependent source models using a log-normal recurrence interval distribution have been developed and improved over the last decade, but studies have generally focused on only a portion of the state.

The U.S. Geological Survey (USGS) first published time-dependent conditional probabilities, and their supporting data, for the San Andreas fault system in California (WGCEP88, 1988). WGCEP88 used the concept of a parametric sigma (σ_p) derived from the uncertainty in the estimate of the mean-recurrence interval for a specific fault, and an intrinsic sigma (σ_i) representing the standard deviation in the natural log-normal distribution of recurrence intervals. Intrinsic sigma represents the inherent randomness in recurrence intervals of characteristic earthquakes on a fault.

*Present address: U.S. Geological Survey, 3876 Central Ave., Suite 2, Memphis, Tennessee 38152-3050.

†Present address: U.S. Geological Survey, P.O. Box 25046, MS-999, Denver, Colorado 80225-0046.

WGCEP88 used $\sigma_i = 0.21$ in computing their conditional probabilities. After the 1989 *M* 7.0 Loma Prieta earthquake, the USGS updated the time-dependent probabilities and information for the San Francisco Bay area (WGCEP90, 1990). Litehiser *et al.* (1992) published a time-dependent PSH model for the San Francisco Bay area and compared time-dependent and time-independent results. Using an intrinsic sigma of 0.21, Litehiser *et al.* found significant differences between time-dependent and Poisson maps at 10% exceedence in 50 years. More recently, the Southern California Earthquake Center (SCEC) published a time-dependent PSH model for southern California (WGCEP94, 1995) using an intrinsic sigma of 0.50 ± 0.20 and found that 10% exceedence in 50-year hazard estimates were not significantly different from their Poisson model. WGCEP94 (1995) also introduced the concept of cascading or combining contiguous fault segments of a major fault into combinations of multisegment rupture earthquakes, as well as single segment rupture earthquakes.

CDMG's responsibilities in reviewing loss assessments affecting public policy led CDMG to develop a statewide time-dependent PSH model based on available consensus information for the purpose of sensitivity testing and consensus discussion. While this paper presents a time-dependent model for California, the goal of this paper is to discuss the consensus and nonconsensus aspects of time-dependent modeling and show the sensitivity of the resulting hazard maps to input parameters. In this article, sensitivity tests show the impact of intrinsic sigma, the degree of cascading, and time-dependence on hazard and expected damage estimates in California, and on PSH model moment-rate budgets.

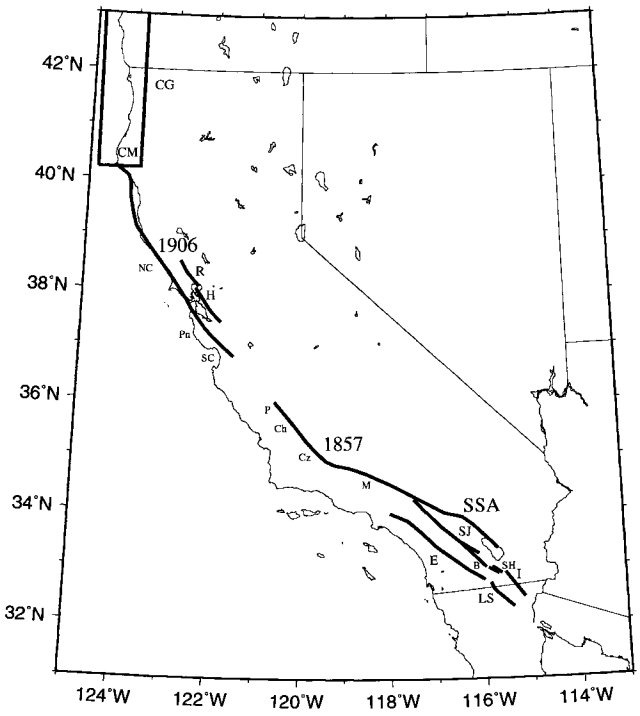

Figure 1. A map showing Type A faults from the CDMG Poisson probabilistic seismic-hazard model. Labeled features include CM, Cape Mendocino; 1906, 1857, and SSA, modeled multisegment ruptures for the 1906, 1857, and postulated southern San Andreas earthquakes; R, Rodgers Creek fault; H, Hayward fault; SJ, San Jacinto fault; E, Elsinore fault; I, Imperial fault; LS, Laguna Salada fault; NC, Pn, SC, P, Ch, Cz, and M, the North Coast, Peninsula, Santa Cruz, Parkfield, Cholame, Carrizo, and Mojave segments of the San Andreas fault; and SH and B, the Superstition Hills and Borego Mountain segments of the San Jacinto fault. The box feature labeled CG represents the dipping portion of the Gorda segment of the Cascadia subduction zone that is also in the CDMG Poisson model as a Type A fault.

Model

The time-dependent PSH models used in this article build on the consensus time-dependent information from the three Working Groups on California Earthquake Probabilities (WGCEP88, 1988; WGCEP90, 1990; WGCEP94, 1995) and on the consensus 1996 CDMG/USGS Poisson PSH model for California (Petersen *et al.,* 1996). The time-dependent elements replace the Type A fault elements of the 1996 CDMG/USGS Poisson PSH model. These Type A faults are shown in Figure 1. Fault geometry and segmentation are the same as in the 1996 CDMG/USGS model. Note that there are some differences between the northern San Andreas fault PSH model of WGNCEP96 (1996) and that of Petersen *et al.* (1996). This article uses the Petersen *et al.* (1996) model as a standard of comparison and hence uses the cascading and fault parameters for the northern San Andreas of Petersen *et al.* in its time-dependent models.

Conditional probabilities were derived in a manner similar to that used by Southern California Earthquake Center (SCEC) (WGCEP94, 1995), with an important distinction. WGCEP94 (1995), in Appendix A, correctly identifies that the log-normal probabilities should be computed using the intrinsic (or aleatory) variability $\sigma_{\ln T}$, which is the standard deviation of the natural logarithm of the random recurrence interval *T*, that is intrinsic sigma. Intrinsic sigma represents the observed aleatory (random) variability in the log-normal variable *T*. In this article, conditional probabilities have been derived only using intrinsic sigma (σ_i) for $\sigma_{\ln T}$. Previous working group reports used the square root of the sum of the squares of both intrinsic and parametric sigma. However, for this article, parameteric sigma represents an epistemic (knowledge or model) uncertainty and intrinsic sigma is an aleatory (random) variability. Parametric sigma (σ_p) is the standard error in the estimate of the mean of *T* and is related to intrinsic sigma by $\sigma_p = \sigma_i/\sqrt{(n)}$, where *n* is the number of recurrence intervals available for estimating the mean-recurrence interval (Savage, 1991, equation 6).

For those few fault segments with a sequence of dated

past characteristic earthquakes (Parkfield, Mojave, and the Gorda segment of the Cascadia subduction zone in this article), the method of Savage (1991) provides estimates of mean-recurrence interval and intrinsic sigma for calculating conditional probabilities. A median-recurrence interval $\hat{T}$ for a sequence of n T_i can be calculated from $\ln \hat{T} = n^{-1} \times \text{sum} \ln T_i$, and its standard deviation can be calculated from $\sigma_i^2 = \sigma_{\ln T}^2 = \text{sum}\{[\ln (T_i/\hat{T})]^2\}/(n-1)$ (Savage, 1991, equations 5 and 9). The mean recurrence interval $\overline{T}$ is derived from the median value $\hat{T}$ by $\overline{T} = \hat{T} \times \exp(\sigma_{\ln T}^2/2)$ (Savage, 1991, equation 2; Benjamin and Cornell, 1970, equation 3.3.34). Note that although Savage (1991) provides a method of calculating the standard error in the estimate of the mean-recurrence interval (parametric sigma), it is not used in the calculation of conditional probabilities (see previous paragraph).

For the remaining time-dependent elements with only one dated characteristic earthquake, conditional probabilities are calculated from an estimate of mean-recurrence interval and the mean value of WGCEP94 for intrinsic sigma (0.5). Specifically, the mean-recurrence interval for a fault segment is estimated from the mean displacement (D) for its characteristic earthquake divided by its mean slip rate (V). Uncertainty in the mean-recurrence interval or parametric uncertainty (σ_p) is calculated from the uncertainties in mean displacement and mean slip rate (assuming that D and V are normally distributed and there is no correlation between them) using the approach of Benjamin and Cornell (1970, p. 184). In this specific case for $f(D,V) = \ln T = \ln (D/V)$,

$$\sigma_P^2 = (f/D)^2\sigma_D^2 + (f/V)^2\sigma_V^2 = (\sigma_D/D)^2 + (\sigma_V/V)^2$$

where T = recurrence interval, D and σ_D are the mean and standard deviation of a fault's characteristic earthquake displacement, and V and σ_v are the mean and standard deviation of that fault's slip rate. Note that σ_p is the epistemic uncertainty in the estimate of the mean-recurrence interval, and it should only be used in a logic-tree analysis to represent possible model variability in the estimate of the mean-recurrence interval.

The conditional probability for a fault segment is then calculated from the exposure period (50 years in this article), mean-recurrence interval, its intrinsic uncertainty, and the elapsed time since the last major earthquake on the segment. This is accomplished by integrating the log-normal probability density function (pdf) for a fault from the elapsed time since the last earthquake to the elapsed time plus the exposure period. The pdf, $f_T(t)$, for a log-normal distribution with a median $\hat{m}$ and intrinsic variability (standard deviation of the natural logarithm of the recurrence interval) $\sigma_{\ln T}$ is

$$f_T(t) = \exp(-(\ln(t/\hat{m})^2/(2\sigma_{\ln T}^2)) \;/\; (t\sigma_{\ln T}\sqrt{2\pi})$$

(see Benjamin and Cornell, 1970, p. 265, equation 3.3.25 and WGCEP94, 1995, Appendix A, equation A1). Please note that in this article we have, by definition, set $\sigma_{\ln T} = \sigma_i$! Intrinsic sigma is the actual variance (standard deviation) of recurrence intervals about the mean-recurrence interval determined from a dated sequence of earthquakes on a fault or as a mean value from a set of σ_i's from other faults around the world. The latest consensus intrinsic sigma mean value of 0.5 (WGCEP94, 1995) was applied to faults with only one dated characteristic earthquake because (1) there is very little data available for California (see Discussion section) and (2) the goal of this article is to understand the sensitivity of results to intrinsic sigma. In calculating the conditional probability, the mean-recurrence interval is converted to the median-recurrence interval using median = mean $\times \exp(-\sigma_{\ln T}^2/2)$ (see Benjamin and Cornell, 1970, p. 266, equation 3.3.34 and WGCEP94, 1995, Appendix A, equation A2).

Table 1 presents the information used to determine the conditional probabilities for a time-dependent PSH model. Conditional probabilities have been calculated using (1) slip rates from the 1996 CDMG/USGS model, (2) displacements from the WGCEP90 (1990) and WGCEP94 (1995) reports, and (3) a mean-intrinsic sigma (σ_i) of 0.5 (WGCEP94, 1995) throughout the state of California unless a fault specific value is available. Table 1 also lists the mean recurrence interval (T-bar), computed parametric uncertainty (σ_p), intrinsic sigma (σ_i) used, and the year of the last earthquake. Note that the mean-recurrence intervals in Table 1 are derived in a different manner than the Poisson mean-recurrence intervals given in Appendix A of Petersen *et al.* (1996) and hence can differ in some cases as shown in Table 1.

Other additional published information was required to compute conditional probabilities for three faults in Table 1 (see footnotes). Sufficient displacement information was not available in the WGCEP90 and WGCEP94 reports for the Parkfield segment of the San Andreas, the Laguna Salada fault, or the Gorda segment of the Cascadia subduction zone. Mean-recurrence interval and uncertainty from Savage (1991), displacement estimates from displacement vs. fault-length relations of Wells and Coppersmith (1994), and mean-recurrence interval and its standard deviation from the paleoseismic tsunami interval data of Valentine *et al.* (1992) were used in determining conditional probabilities for these three faults. Additionally, the date of the last event on the northern Hayward fault has been changed from the WGCEP90 value based on Toppozada and Borchardt's (1998) conclusion that the 1836 event did not occur on the northern Hayward fault.

The resulting 50-year-conditional probabilities for $\sigma_i = 0.50$ are listed in Table 2 along with Poisson 50-year probabilities based on annual rates from Petersen *et al.* (1996). Note that actual observed σ_is are held fixed for the Parkfield (0.35), Mojave (0.77), and Gorda (0.43) segments (see footnotes to Table 1). A comparison of time-dependent and Poisson probabilities shows the effect on probabilities of the time-dependent assumption for Type A faults. Generally, but not always, time-dependence raises the probabilities except for those segments and ruptures that have had earthquakes recently (e.g., the Santa Cruz segment, the 1906 rupture, the

Table 1

Time-dependent Fault Segments and their Slip Rates (mm/yr), Displacements (m), Recurrence Intervals (T-bar) (yrs), Parametric Uncertainty (σ_p), Intrinsic Sigma (σ_i), and Year of Last Earthquake (LastEqk)*

Fault Segment	Slip Rate	Displacement	*T*-bar	+	−	σ_p	σ_i	LastEqk
San Andreas:								
Coachella	25.00 ± 5.00	4.00 ± 3.00†	160##	189	87	.39†	.50	1690
San Bernardino	24.00 ± 6.00	3.50 ± 1.00	146	67	46	.19	.50	1812
Mojave	30.00 ± 7.00	4.50 ± 1.50	135‡	92	55	.26‡	.77‡	1857
Carrizo	34.00 ± 3.00	7.00 ± 4.00	206	162	91	.29	.50	1857
Cholame	34.00 ± 5.00	4.75 ± 4.00	140	191	81	.43	.50	1857
Parkfield	34.00 ± 5.00	0.75 ± 0.12§	22§	8	5	.16§	.35§	1966
Santa Cruz	14.00 ± 3.00	1.60 ± 0.60	114##	63	41	.22	.50	1989
Peninsula	17.00 ± 3.00	2.60 ± 1.00	153##	80	52	.21	.50	1906
North Coast	24.00 ± 3.00	4.50 ± 1.00	188##	56	43	.13	.50	1906
Imperial	20.00 ± 5.00	1.20 ± 0.80	60	61	30	.35	.50	1979
San Jacinto:								
Superstition Hills	4.00 ± 2.00	1.00 ± 0.30	250	197	110	.29	.50	1987
Superstition Mtns	5.00 ± 3.00	2.00 ± 0.30	400##	343	185	.31	.50	1430
Borego Mtn	4.00 ± 2.00	0.70 ± 0.20	175	138	77	.29	.50	1968
Coyote Creek	4.00 ± 2.00	0.70 ± 0.30	175	164	85	.33	.50	1892
Anza	12.00 ± 6.00	3.00 ± 1.00	250	197	110	.29	.50	1750
San Jacinto Valley	12.00 ± 6.00	1.00 ± 0.20	83	59	35	.27	.50	1918
San Bernardino	12.00 ± 6.00	1.20 ± 0.30	100	75	43	.28	.50	1890
Laguna Salada	3.50 ± 1.50	1.00 ± 0.30‖	286##	195	116	.26	.50	1892
Elsinore:								
Coyote Mtn	4.00 ± 2.00	2.50 ± 0.50	625	448	261	.27	.50	1892
Julian	5.00 ± 2.00	1.70 ± 0.20	340	177	117	.21	.50	1892
Temecula	5.00 ± 2.00	1.20 ± 0.30	240	148	91	.24	.50	1818
Glen Ivy	5.00 ± 2.00	1.60 ± 0.40	320##	197	122	.24	.50	1910
Whittier	2.50 ± 1.00	1.90 ± 0.20	760##	397	261	.21	.50	650
Hayward:								
Hayward-all#	9.00 ± 1.00	1.50 ± 1.00	167	163	82	.34	.50	<1776**
Hayward-S#	9.00 ± 1.00	1.50 ± 1.00	167	163	82	.34	.50	1868
Hayward-N#	9.00 ± 1.00	1.50 ± 1.00	167	163	82	.34	.50	<1776**
Rodgers Creek	9.00 ± 2.00	2.00 ± 1.00	222	159	93	.27	.50	<1808
Cascadia-Gorda	35.00 ± 5.00	8.50 ± 3.00††	437‡‡	141	107	.14‡‡	.43‡‡	1700§§

*Listed uncertainties are 2σ, except σ_p and σ_i. Slip rates are taken from Petersen (1996) and displacements and last earthquakes are taken from WGCEP90 (1990) and WGCEP94 (1995) unless otherwise indicated. σ_p is calculated from the standard deviations (σ_V and σ_D) of mean slip rate (m_V) and mean displacement (m_D) using the formula $\sigma_p = \sqrt{(\sigma_V/m_V)^2 + (\sigma_D/m_D)^2}$ (see text). The uncertainties in *T*-bar are calculated using σ_p and are $2\sigma_p$ uncertainties.

##Indicated mean-recurrence intervals differ from Appendix A of Petersen *et al.* (1996) because displacement values were not used by Petersen *et al.* in their Poisson methodology.

†WGCEP94 (1995) lists a 4.0 + 4.0 − 2.0 m displacement. But σ_p is calculated using a displacement 2σ of 3.0m.

‡Mean-recurrence interval, intrinsic sigma, and parametric sigma calculated from the paleoseismic data of Sieh *et al.* (1989) using the method of Savage (1991). Best-estimated dates of Sieh *et al.* of earthquake occurrence as listed in their Table 3 (p. 614) were used in the calculation.

§Displacements are not given by the Working Groups. Savage (1991) gives a median *T* of 20.9 and a σ_i of .35. T-bar was determined from Savage's median *T*, and σ_p was estimated from Savage's Parkfield earthquake recurrence intervals listed in his Table 1 (p. 866). Because Savage's is the most recent Parkfield recurrence analysis, *T*-bar and σ_p based on his results are used to estimate the displacement given here.

‖Displacement is estimated from Wells and Coppersmith's (1994) average displacement equation for strike-slip faults using an $M = 7$ characteristic earthquake. Uncertainty is arbitrary but similar to that of other San Jacinto and Elsinore segments.

#The Hayward fault model by Petersen *et al* (1996) is not a cascade model but a model that states that half the time the Hayward fault ruptures as individual segments and half the time as a rupture of both segments together (see their pages 12 and A-2).

**Toppozada and Borchardt (1998) showed that the 1836 earthquake thought to be on the northern Hayward really occurred east of Monterey Bay. This is a change since WGCEP90 (1990).

††Displacement is estimated from Wells and Coppersmith's (1994) average displacement equation for all faulting types using an $M = 8.3$ characteristic earthquake (the reverse faulting equation is too poorly constrained). Uncertainty is arbitrary but unimportant.

‡‡T-bar calculated from the given displacement and slip rate (243 years) does not match the seismic history and paleoseismicity of the Cascadia subduction zone. Valentine *et al.* (1992) provide a sequence of paleotsunami dates that can be used to estimate a mean-recurrence interval, intrinsic sigma, and parametric sigma via the method of Savage (1991).

§§Based on the recent Japanese tsunami results by Satake *et al.* (1996) and Washington and Oregon dendochronology by Jacoby *et al.* (1997).

Superstition Hills segment, the Borego Mtn. segment, etc.). The effect of time-dependence on hazard is shown in the Sensitivity Tests section below.

PSH estimates need to be made and combined for both the time-dependent faults (Type A faults) and the Poisson faults plus background seismicity (Type B & C faults plus background areal sources) that make up the entire time-dependent PSH model. This was done by calculating hazard

Table 2
Rates and Probabilities for Preferred CDMG Poisson and Time-Dependent PSH Models*

Fault Segment or Cascade	Poisson Annual Rate	Poisson 50-Year Probability	Time-Dependent 50-Year Probability
San Andreas:			
Southern Rupture	0.00454	0.203	0.471
Coachella	0.00000	0.000	0.000
San Bernardino	0.00231	0.109	0.076
1857 Rupture	0.00485	0.215	0.338
Mojave	0.00182	0.087	0.075
Carrizo	0.00000	0.000	0.000
Cholame	0.00229	0.108	0.269
Parkfield	0.04060	0.869	0.999
1906 Rupture	0.00476	0.212	0.151
Santa Cruz	0.00250	0.118	0.000
Peninsula	0.00250	0.118	0.307
North Coast	0.00000	0.000	0.171
Imperial:	0.01258	0.467	0.704
San Jacinto			
Superstition Hills	0.00400	0.181	0.006
Superstition Mtns	0.00200	0.095	0.231
Borego Mtn	0.00571	0.248	0.098
Coyote Creek	0.00571	0.248	0.366
Anza	0.00400	0.181	0.328
San Jacinto Valley	0.01205	0.453	0.709
San Bernardino	0.10000	0.393	0.645
Laguna Salada	0.00297	0.138	0.134
Elsinore:			
Coyote Mtn	0.00160	0.077	0.005
Julian	0.00294	0.137	0.080
Temecula	0.00417	0.188	0.308
Glen Ivy	0.00294	0.137	0.068
Whittier:	0.00156	0.075	0.128
Hayward:			
Hayward-all (50%)	0.00300	0.139	0.269
Hayward-S (50%)	0.00300	0.139	0.242
Hayward-N (50%)	0.00300	0.139	0.269
Rodgers Creek:	0.00450	0.201	0.348
Cascadia:			
Gorda (67%)	0.00445†	0.199	0.170
Full (33%)	0.00066	0.032	0.000

*The Poisson model rates are from Petersen *et al.* (1996). The time-dependent model used $\sigma_i = 0.50$. All listed probabilities are for a 50-year exposure time (starting in 1999) and all listed rates are annual rates. Only the San Andreas has cascaded segments in these models in conformity with Petersen *et al.* (i.e., southern, 1857, and 1906 ruptures, which incorporate into one rupture the segments listed after their entry in the table). The remaining entries are single-segment ruptures in these models, which in the case of the San Andreas handles the remaining moment rate release left over from the cascade portion of the model (see text for details).

†The CDMG/USGS Poisson model uses a floating *M* 8.3 rupture along the Cascadia subduction zone with this Poisson annual rate; see Petersen *et al.* (1996) or Frankel *et al.* (1996).

curves directly from 50-year probabilities. For the Poisson elements of the model, annual rates of occurrence (λ) were converted to 50-year probabilities (P_{50}) prior to hazard calculations using $P_{50} = 1 - e^{-\lambda t}$, where $t = 50$ years.

Recently, Thatcher *et al.* (1997) examined fault displacements for the 1906 rupture of the northern San Andreas fault and reviewed the arguments about whether the 1989 Loma Prieta earthquake affected the conditional probability of the Santa Cruz segment of the San Andreas fault. First, Thatcher *et al.* indicate that fault displacements at depth in 1906 were up to two-times larger than the 1906 surface displacements used by WGCEP90 (1990). They suggested that 30-year conditional probabilities for the northern San Andreas would be 5–10% lower and would have some impact on hazard calculations. However, our results suggest that such small changes in conditional probabilities would have little impact on PSH calculations (see Table 2 and Sensitivity Tests section)

The second point, which is of larger concern, is whether the 1989 Loma Prieta earthquake reset the conditional probability clock on the Santa Cruz segment of the San Andreas fault as assumed by WGCEP90, or not as suggested by Thatcher *et al.* (1997). Not resetting the conditional probability clock would make the probability higher on the Santa Cruz segment of the San Andreas fault. The PSH models presented in this article have used the consensus values of WGCEP90, but it is acknowledged that Thatcher *et al.* (1997) could change that consensus in the near future.

Discussion

Nonconsensus Aspects

While most of the time-dependent PSH models presented in this article are based on consensus information for California, consensus has not been reached on some aspects incorporated into them, as described in Table 1. Also some of the consensus values are seven years old and will be revised by a 1999 working group on northern California earthquake probabilities. There are four areas where these time-dependent models are potentially controversial: (1) the value of intrinsic sigma, (2) segmentation and the amount of cascading, (3) the selection of faults that are modeled with time-dependence (e.g., the application of time-dependence on fault segments that WGCEP94 treated with a Poisson model), and (4) the assumption of a log-normal distribution of recurrence intervals as opposed to other distributions such as the Brownian Passage Time, Weibull, Gamma, etc. The sensitivity of hazard to the use of alternative recurrence-interval distributions is discussed by Ellsworth *et al.* (1999). Ellsworth *et al.* find that it is not possible to discriminate among candidate distributions because the existing world-wide earthquake recurrence interval data are too limited in number per sequence and uncertain in event dating. The remaining three aspects will be discussed in this section and the results of sensitivity tests will be presented in the following section of this article.

Intrinsic Sigma. Intrinsic sigma is the overall uncertainty (standard deviation) in the natural logarithm of the recurrence intervals, and it describes how regularly or irregularly characteristic earthquakes are expected to occur on any time-dependent fault. An intrinsic sigma near zero indicates the very regular occurrence of characteristic earthquakes such as occurred on the Parkfield segment of the San Andreas fault from 1857 to 1922 (Bakun and McEvilly, 1984). Note

that the coefficient of variation (cov) of a log-normal distribution, which is σ_T/m_T (standard deviation of T over the arithmetic mean of T), is related to it's intrinsic variability (intrinsic sigma) by $\sigma^2_{\ln T} = \ln(\mathrm{cov}_T^2 + 1)$ (Benjamin and Cornell, 1970, p. 266, equation 3.3.35).

Intrinsic sigma has been the subject of much discussion. WGCEP88 (1988) and WGCEP90 (1990) used an intrinsic sigma of 0.21 based on a worldwide set of cov's for earthquake recurrence intervals on plate-boundary faults by Nishenko and Buland (1987). Savage (1991) criticized the use of such a small intrinsic sigma, which implies a small deviation in recurrence intervals between characteristic earthquakes from the mean-recurrence interval. Savage also pointed out limitations in the use of a log-normal distribution to model characteristic earthquake occurrences. WGCEP94 (1995) chose to use an intrinsic sigma of 0.50 $\pm$ 0.20 in southern California. And Ellsworth *et al.* (1999) found from statistical tests that (1) the limited worldwide earthquake recurrence interval data have a Brownian Passage Time model (very similar to log-normal) shape factor (basically the cov of the distribution) of 0.46 $\pm$ 0.32, (2) the 35 recurrence interval sequences examined are compatible with a shape factor of 0.50, and (3) the 35 earthquake sequences had no systematic differences when grouped by tectonic style.

Actual data on which to estimate intrinsic sigma in California are sparse. Nishenko and Buland (1987) indicate a cov of 0.33 for the Parkfield segment and 0.29 for Pallett Creek paleoseismic data (Mojave segment), using a criterion of at least four earthquake recurrence intervals on a fault segment to estimate total variability. Savage (1991) indicates a total variability of 0.35 for the Parkfield segment. Those are all the published estimates of total variability values for California and they are from the San Andreas, a major strike-slip fault. In this article, an intrinsic sigma of 0.77 is obtained from the mean values for the revised and larger Pallet Creek paleoseismic data set of Sieh *et al.* (1989). The paleoseismic data from tsunami deposits presented by Valentine *et al.* (1992) for the southern end of the Cascadia subduction zone suggest an intrinsic sigma of about 0.43 based on nine weakly constrained recurrence intervals. This value is larger than Nishenko and Buland's values for subduction zones.

For this article and the purpose of sensitivity testing, the WGCEP94 (1995) intrinsic sigma mean value of 0.50 was adopted statewide unless fault-specific intrinsic sigma's were available. Although alternative interpretations for California could be based on the few actual data for California (say an intrinsic sigma of 0.35 for strike-slip faults and about 0.40 for the Cascadia subduction zone), the small number of recurrence intervals in California sequences (<10), the arguments of Savage (1992), and the analysis of Ellsworth *et al.* (1999) suggest that a statewide intrinsic sigma of 0.5 is the most defensible choice. The effect of varying intrinsic sigma is investigated in the following Sensitivity Tests section.

Cascading. Contiguous segments of a major fault can rupture together producing a larger cascaded earthquake, as well as rupture separately in smaller earthquakes. The 1857 earthquake on the San Andreas fault is an example of a multisegment rupture involving the Parkfield, Cholame, Carrizo, and Mojave segments, and the 1966 Parkfield earthquake is an example of a single-segment rupture. PSH models can allow for multisegment, contiguous ruptures by cascading modeled segments into larger earthquakes using slip rates, recurrence rates, or conditional probabilities. This cascading of segments into larger magnitude earthquakes affects the moment-rate budget of the PSH model (sum of the products of each earthquake's seismic moment and annual rate of occurrence) and hence hazard by removing the need for a larger number of moderate-sized earthquakes to balance the moment rate in the PSH model.

Different working groups have cascaded segments in different ways. WGCEP94 (1995) chose to cascade segments for the San Andreas, San Jacinto, and Elsinore fault systems in southern California, but also had an alternative noncascade model. Cramer *et al.* (1996) showed no significant difference in 10% probability of exceedence in 50-year hazard between the WGCEP94 cascade and noncascade models. Petersen *et al.* (1996) chose only to cascade those segments of the San Andreas corresponding to the 1857 and 1906 ruptures plus a postulated southern San Andreas rupture, and left any remaining moment rate on individual segments. The cascading approach of Petersen *et al.* (1996) was adopted for this article.

Cascading of individual segments into longer ruptures can be done in many ways. The extremes can be represented as no cascading (moment rate on an individual segment is released only by characteristic earthquakes on that segment) and full cascading (moment rates for individual segments are released by the longest multisegment ruptures with the largest moment rates possible while avoiding the transfer of moment rate from one segment to another). In full cascading all potential combinations of contiguous segment ruptures are considered and multisegment rupture rates are maximized. But moment-rate redistribution among the segments being cascaded (that is, moment rate redistribution along the fault) is not allowed in this definition of full cascading. Redistributing moment-rate release along a fault, by averaging or other means, will cause larger changes in hazard than the full cascading discussed in this article (see Cramer *et al.,* 1996, Figure 9). The cascading used by Petersen *et al.* (1996) and in this article is a partial cascade between these extremes but accounts for a majority of the moment rate of full cascading. The effect of cascading on hazard and moment-rate budget is investigated in the Sensitivity Tests section.

Cascading fault segments into a multisegment rupture can be accomplished by slip rate, recurrence rate, or conditional-probability cascading. Because all these approaches are based on conserving moment rate for each cascaded segment, the hazard results are essentially the same. In this article, adjacent segments are cascaded using their conditional probabilities. This is accomplished by using the following relation between a given segment's conditional probability

($P\mathrm{s}_i$) and the probabilities ($P\mathrm{c}_j$) of that segment participating in a set of multisegment and individual ruptures:

$$1 - P\mathrm{s}_i = \Pi_j (1 - P\mathrm{c}_j).$$

Ps_i is known for each segment i, but there are many ways of partitioning probability (moment rate) to a set of multisegment and individual ruptures. A further constraint on the probability (moment rate) distribution among a set of multisegment and individual ruptures is required to obtain a unique solution. As previously stated, in this article we have maximized the probability (rate) of multisegment ruptures. This is illustrated in Table 3.

Time-Dependence. A goal of this article is to examine the effect time-dependence has on PSH values within California compared to time-independence. WGCEP94 (1995) found little difference in hazard between their preferred time-dependent model and their alternative Poisson model. WGCEP94 changed the Parkfield and Cholame segments of the San Andreas and the Imperial fault from time-dependent (WGCEP88, 1988) to Poisson segments, because of concerns about noncharacteristic behavior or large uncertainties in the data used to determine time-dependent behavior. The Poisson model by Petersen *et al.* (1996) treated these three fault segments as Type A faults (characteristic behavior only). Petersen *et al.* also treated the Laguna Salada fault and the Gorda segment of the Cascadia subduction zone as Type A faults. For consistency and in order to make comparisons, the time-dependent PSH models of this paper retain the Type A fault designations of Petersen *et al.,* but with all Type A faults characterized as time-dependent. The impact of time-dependence versus time-independence on hazard and moment rate budget is investigated further in the following Sensitivity Tests section.

Sensitivity Tests

Sensitivity tests can show the impact of intrinsic sigma, cascades vs. no cascades, and time-dependence vs. time-independence on the results of PSH modeling. Comparisons have been made at arbitrary probabilities of occurrence (P) of 0.021, 0.0021, and 0.0002 (65%, 10%, and 1% probability of exceedence in 50 years or return periods of 63, 475, and 4975 years, respectively). Additionally, expected damage maps are compared after they are calculated using the entire hazard curve as described in Cao *et al.* (1999) and using the ATC-13 facility class 1 vulnerability relation for low-rise, wood frame structures (Applied Technology Council, 1985). Cao *et al.* compute expected annual damage by directly integrating over acceleration and intensity the conditional probability density functions for peak-ground acceleration (from a site's hazard curve), intensity depending on acceleration (Trifunac and Brady, 1975), and damage depending on intensity (Applied Technology Council, 1985). Comparisons are also made among moment-rate budgets for the CDMG Poisson PSH model and the sensitivity test models. For the sensitivity tests, comparisons have been made with intrinsic sigma set to 0.2, 0.3, 0.4, and 0.5, because this is the range where hazard and expected damage are most sensitive to the value of intrinsic sigma. These comparisons have been made by simply taking the ratio of alluvial PGA values or expected damage estimates for two versions of the PSH model that are identical except for the parameter of interest.

Cascading. Figures 2–5 show the results for full cascading vs. no cascading on the San Andreas fault in California (see previous sections for meaning of full cascading). Each figure shows the ratio where differences exceed 0.05 g or \$0.50/thousand from using four separate fixed values of intrinsic sigma. Notice that intrinsic sigma has little influence on the results in each figure. Going from Figure 2 to Figures 3 and 4, ratios in PGA between the indicated models change from few areas with differences exceeding 10% at $P = 0.021$ (65% exceedence in 50 years), to larger areas at $P = 0.0021$ (10% exceedence in 50 years) and $P = 0.0002$ (1% exceedence in 50 years). This increasing difference in PGA at longer return periods (low probability of occurrence) is probably due to the magnification of small-modeling differences. Ratios exceeding a 20% change in annual expected damage

Table 3

An Example of Cascading the Northern San Andreas in California using Conditional Probabilities ($\sigma_i = 0.50$) and Maximizing the Rate of Occurrence of Multisegment Ruptures

Cascade or Segment	i	j	Ps_i	1st Adjustment $1-(1-\mathrm{Ps}_i)/(1-\mathrm{Pc}_1)$	Partial Cascade Pc_j	2nd Adjustment $1-(1-\mathrm{Ps}_i)/[(1-\mathrm{Pc}_1)(1-\mathrm{Pc}_2)]$	Full Cascade Pc_j
1906 rupture		1			.15063		.15063
Penin/NCoast		2			.00000		.17144
Santa Cruz	1	3	.15063	1–(1–.15063)/(1–.15063) =	.00000		.00000
Peninsula	2	4	.41159	1–(1–.41159)/(1–.15063) =	.30723	1–(1–.41159)/(1–.15063)/(1–.17144) =	.16389
North Coast	3	5	.29625	1–(1–.29625)/(1–.15063) =	.17144	1–(1–.29625)/(1–.15063)/(1–.17144) =	.00000

*Ps_i are the conditional probabilities for each individual segment i involved in the cascading process. Pc_j are the probabilities for each rupture j of a set of cascades that includes multisegment and single segment ruptures. The rate of occurrence of a multisegment rupture is maximized by transferring the lowest, nonzero probability of the segments involved to the multisegment rupture and cascading the longest multisegment rupture first (the 1906 rupture in this example).

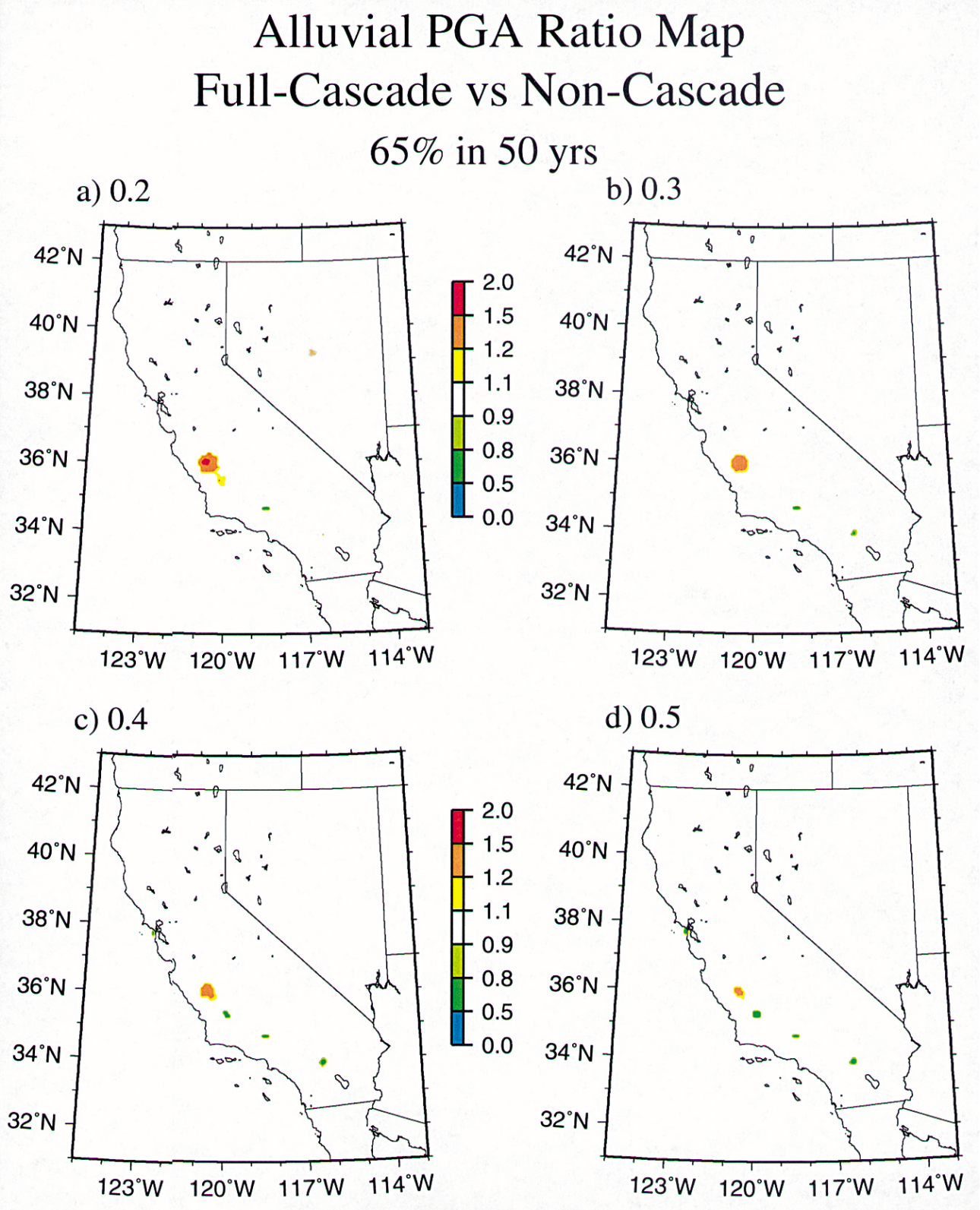

Figure 2. Maps of ratios of alluvial PGA hazard between time-dependent models using full cascading and noncascading along the San Andreas fault system (see text for definitions of cascading). Maps show ratios (full over no cascading) for 65% exceedence in 50-year hazard (63 year return period) using different intrinsic sigmas: (a) 0.2, (b) 0.3, (c) 0.4, and (d) 0.5.

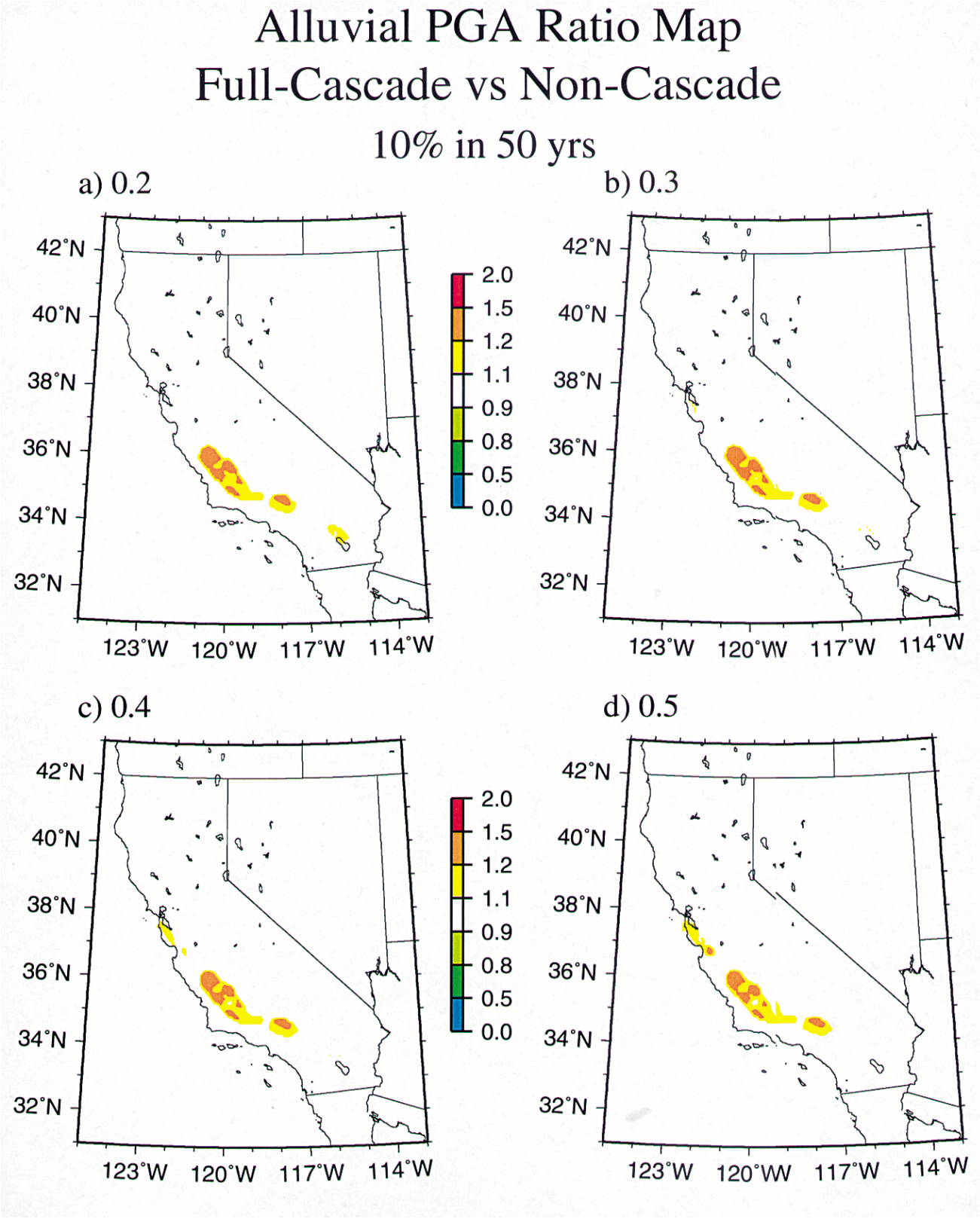

Figure 3. Same as Figure 2 except for a 10% exceedence in 50-year hazard (475-year-return period).

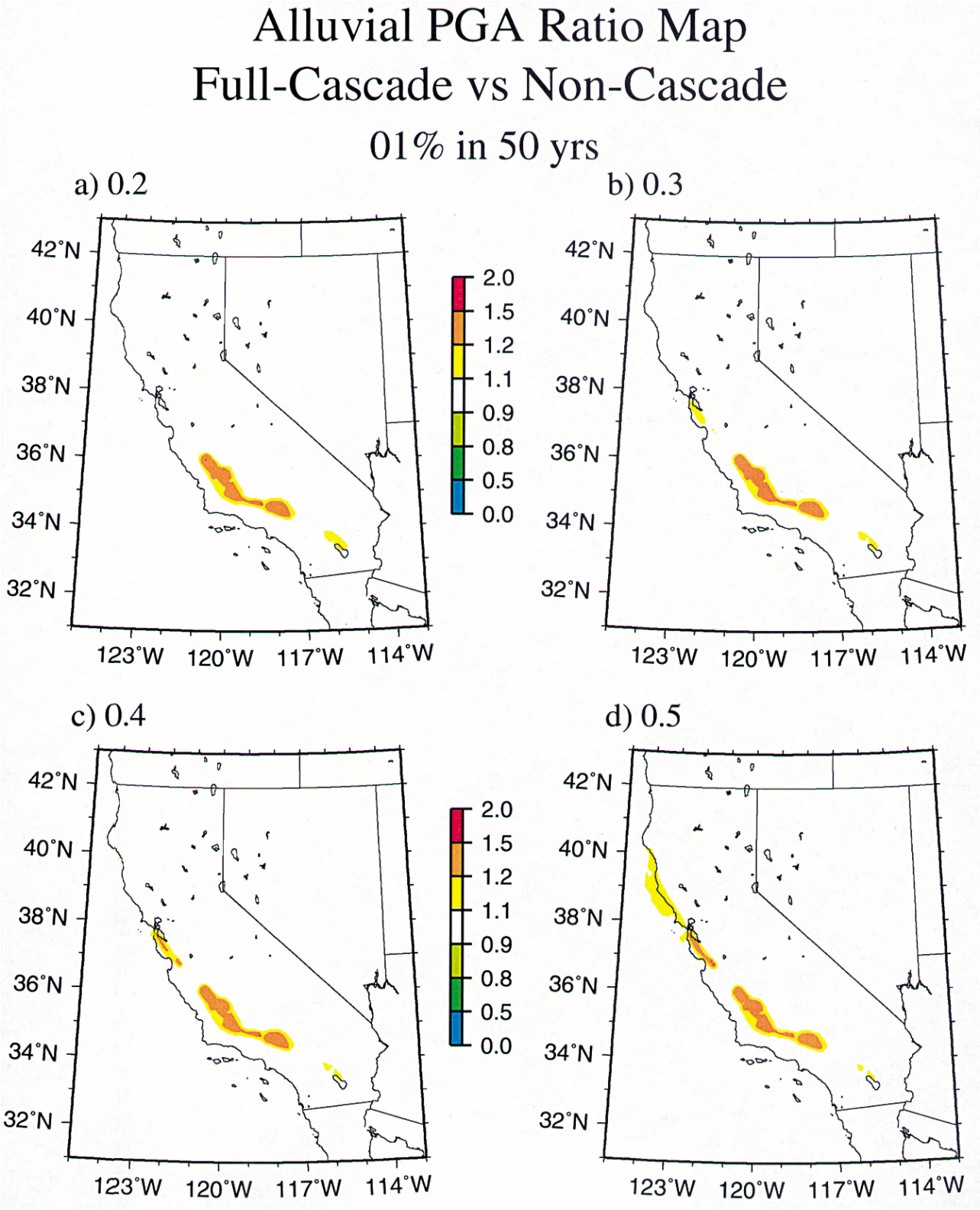

Figure 4. Same as Figure 2 except for a 1% exceedence in 50-year hazard (4975-year-return period).

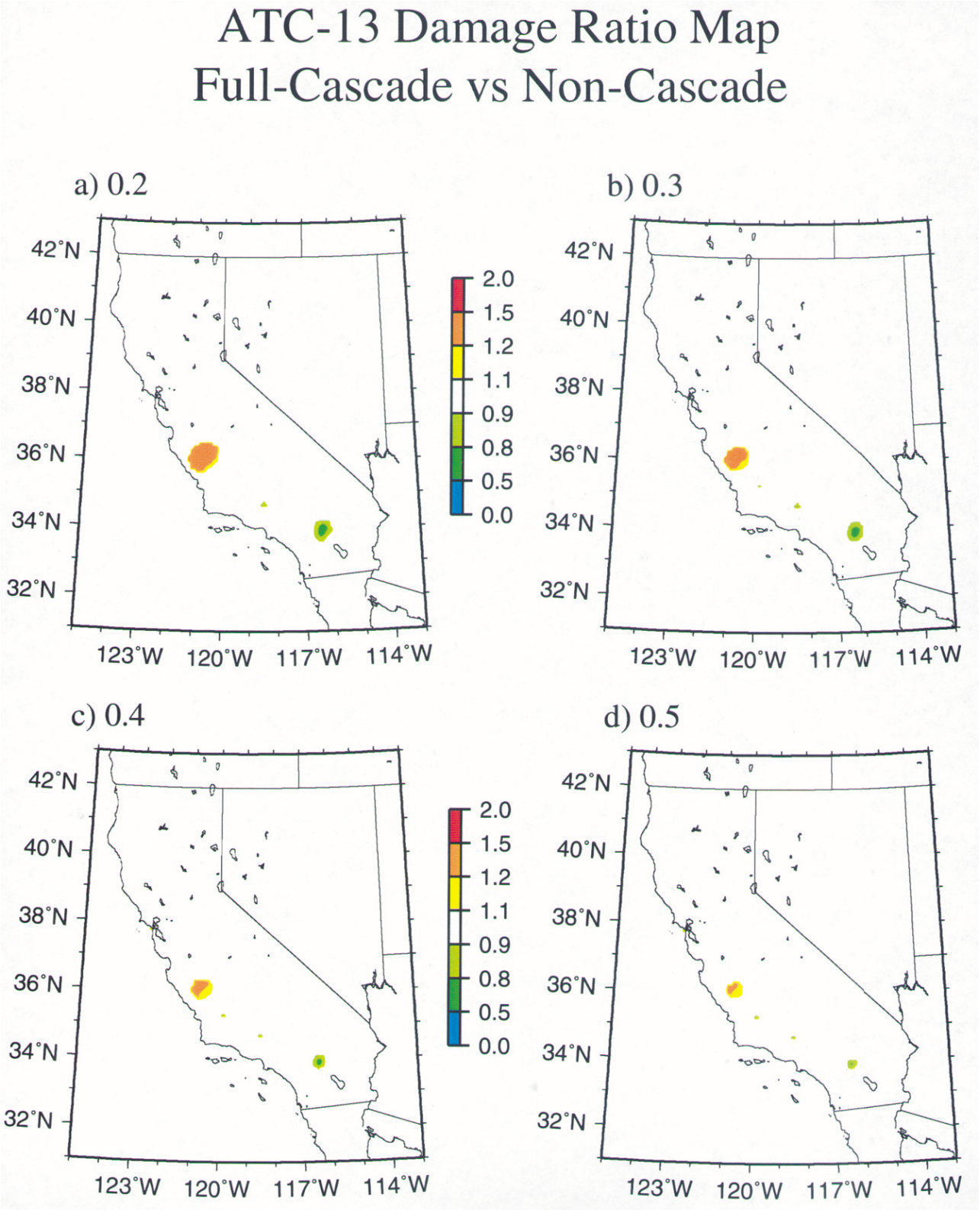

Figure 5. Maps of ratios of expected-damage estimates from alluvial PGA hazard curves between time-dependent models using full cascading and noncascading along the San Andreas fault system (see text). The presentation is as in Figure 2.

estimates (where differences exceed \$0.50/thousand) also effect very small portions of the state—mostly the Parkfield area (Figure 5). Annual expected damage estimates are influenced more by earthquakes with higher probabilities of occurrence (shorter return periods) (Petersen *et al.,* 1997; Cao *et al.,* 1999).

The amount of cascading in the preferred PSH models (time-dependent and Poisson) falls between the extremes of full and no cascading used in Figures 2–5. Thus, differences for either of the preferred PSH models and their respective full or no cascaded versions would be less than that shown in Figures 2–5.

Time-Dependence. Figures 6–9 show the sensitivity comparisons between various time-dependent PSH models presented in this article and the Petersen *et al.* (1996) Poisson PSH model. The amount of cascading and the fault segmentation have been held fixed between time-dependent and Poisson models (with the exception of the Cascadia subduction zone) so that differences are only due to the use of time-dependence on Type A faults, which are assumed to have 100% characteristic earthquake behavior. As in Figures 2–5, Figures 6–9 show ratios where differences exceed 0.05 *g* or \$0.50/thousand for four separate fixed-values of intrinsic sigma. As expected, PGA and expected-damage estimates increase with decreasing intrinsic sigma. An intrinsic sigma of 0.5 shows changes generally less than 20% in Figures 6d–8d, except for the Cascadia subduction zone. An intrinsic sigma of 0.2 shows changes greater than 20% in Figures 6a–8a, usually within 20 km of the Type A faults. The comparison for the Cascadia subduction zone is meaningless because it is influenced by the use of a more complex rupture model in the Poisson PSH model, which is not amenable to a time-dependent approach (see Frankel *et al.,* 1996 and Petersen *et al.,* 1996, for details) as opposed to a single rupture model in the time-dependent PSH models of this article.

Focusing on the strike-slip Type A faults in California shown in Figure 1 (i.e., south of Cape Mendocino), most changes larger than 10% are generally within 20 km of these faults in Figures 6–9. In Figures 6–9 the choice of intrinsic sigma (σ_i) generally creates small areas where the change is greater than 10% when $\sigma_i = 0.4$ and 0.5 and larger areas where change is greater than 10% when $\sigma_i = 0.2$ and 0.3. With decreasing probability of occurrence P (increasing return period) going from Figure 6 to Figure 7 to Figure 8, the size of these areas initially increases from $P = 0.0210$ to $P = 0.0021$ and than decreases from $P = 0.0021$ to $P = 0.0002$. This comes about because absolute differences in PGA always increase with increasing return period but in Figure 8 the absolute values in PGA have increased so much that the ratio actually decreases. For expected damage and PGA hazard at a probability of occurrence of 0.0021 (return periods of 475 years) or less, differences due to time-dependence vs. time-independence only become greater than 20% for $\sigma_i \leq 0.4$ within 20 km of a Type A fault. But for $\sigma_i \geq 0.50$ differences are still generally less than 20% even at a 0.0002 probability of occurrence (4975-year-return period).

An illustration of how intrinsic sigma affects time-dependent results is given in Figure 10. Figure 10 shows the 50-year-conditional probabilities for the North Coast segment of the San Andreas as a function of elapsed time since the last earthquake for an intrinsic sigma of 0.21 and 0.50. For comparison, the Poisson probability is also shown in Figure 10. Generally, the conditional probability for an intrinsic sigma of 0.50 is closer to the fixed Poisson probability than the conditional probability for an intrinsic sigma of 0.21. Also the conditional probability for an intrinsic sigma of 0.50 rises above the Poisson probability level earlier in the recurrence cycle than the conditional probability for an intrinsic sigma of 0.21. This is because an intrinsic sigma of 0.50 indicates a characteristic earthquake-occurrence pattern much closer to Poissonian behavior and an intrinsic sigma of 0.21 indicates a characteristic earthquake-occurrence pattern that is fairly regular in time.

Longer Period Ground Motions. The small variation in alluvial PGA hazard between time-dependent and Poisson PSH models and between previously discussed cascade and noncascade PSH models does not hold for longer period ground motions (1.0 second and greater). This is illustrated in Figure 11 for alluvial spectral acceleration (*Sa*) at 2.0 seconds. Only the $\sigma_i = 0.20$ and 0.50 at 10% exceedence in 50 year results are shown in Figure 11. The colored areas (ratios in ground motion exceeding a 10%) in Figure 11 are larger than the corresponding colored areas of Figures 3 and 7, indicating larger differences at 2-sec Sa.

Moment-Rate Budget. Time-dependence and cascading affect the moment-rate budget of a PSH model. Both calculations start with the same basic long-term seismic-moment rate in the model. Time-dependence mostly affects the short-term rate of the large earthquakes via the choice of intrinsic sigma (as illustrated in Figure 10) and hence the short-term seismic-moment rate for a fault segment. On the other hand, cascading mostly affects the magnitude of the earthquakes included in the model and hence the seismic moment of those earthquakes. This is demonstrated in Table 4, which shows the short-term annual moment-rate budget for the Type A faults from several PSH models used in this article (excluding the moment-rate contribution from the Cascadia subduction zone). The Type A faults account for about half of the moment rate of the entire model when the Cascadia subduction zone is excluded from the moment rate calculations (see caption of Table 4).

The $\sigma_i = 0.50$ time-dependent PSH model has a 41% larger Type A fault short-term moment-rate budget than the CDMG Poisson model of Petersen *et al.,* 1996 (Table 4). Yet Figures 6d–9d generally only show a 20% or less change in PGA hazard and expected-damage estimates along the San Andreas fault. By simply decreasing intrinsic sigma to 0.20, the Type A fault short-term moment-rate budget be-

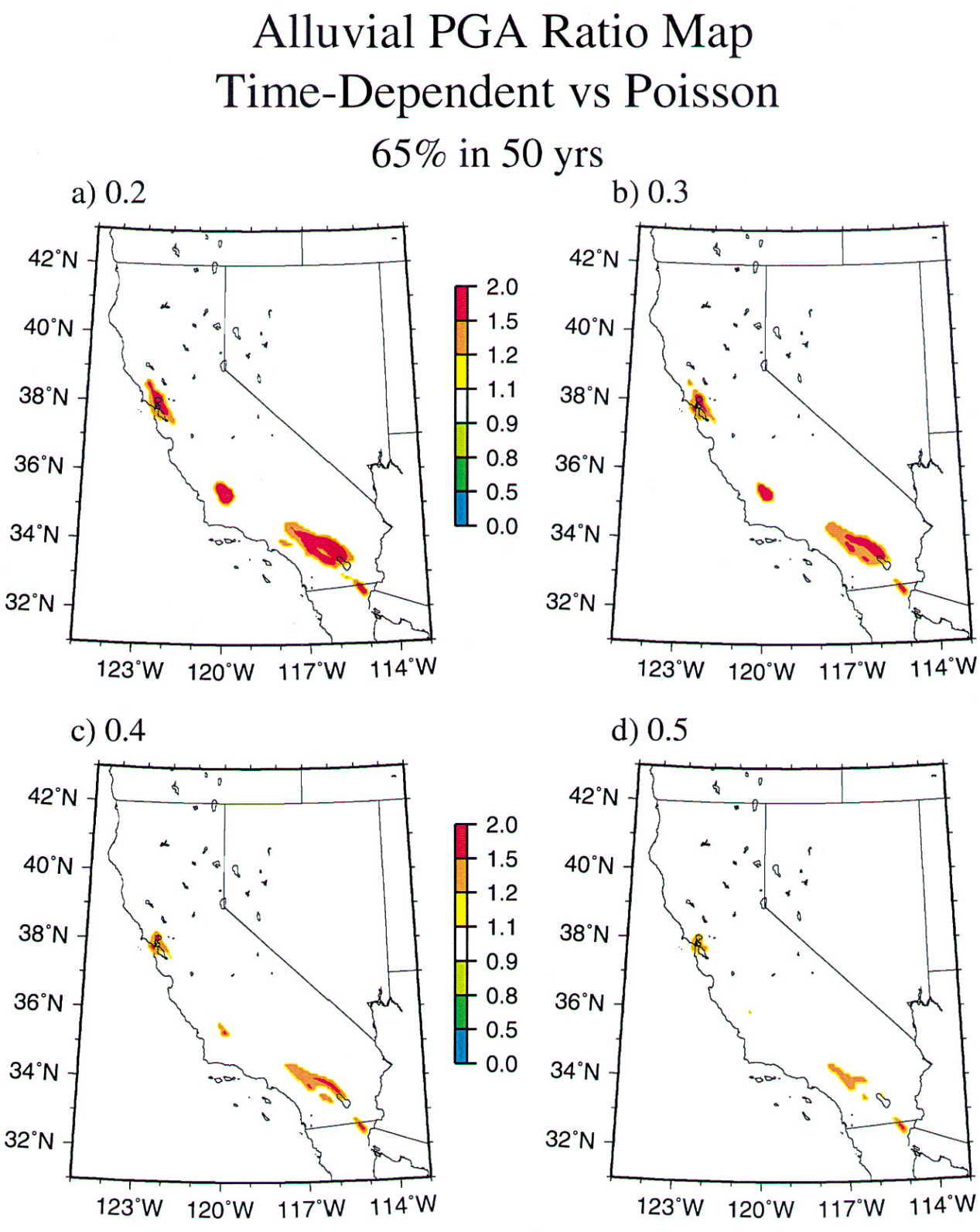

Figure 6. Maps of ratios of alluvial PGA hazard between time-dependent and Poisson models using the same cascading along the San Andreas fault system (see text). Maps show ratios (time-dependent over Poisson) for 65% exceedence in 50-year hazard using different intrinsic sigmas: (a) 0.2, (b) 0.3, (c) 0.4, and (d) 0.5.

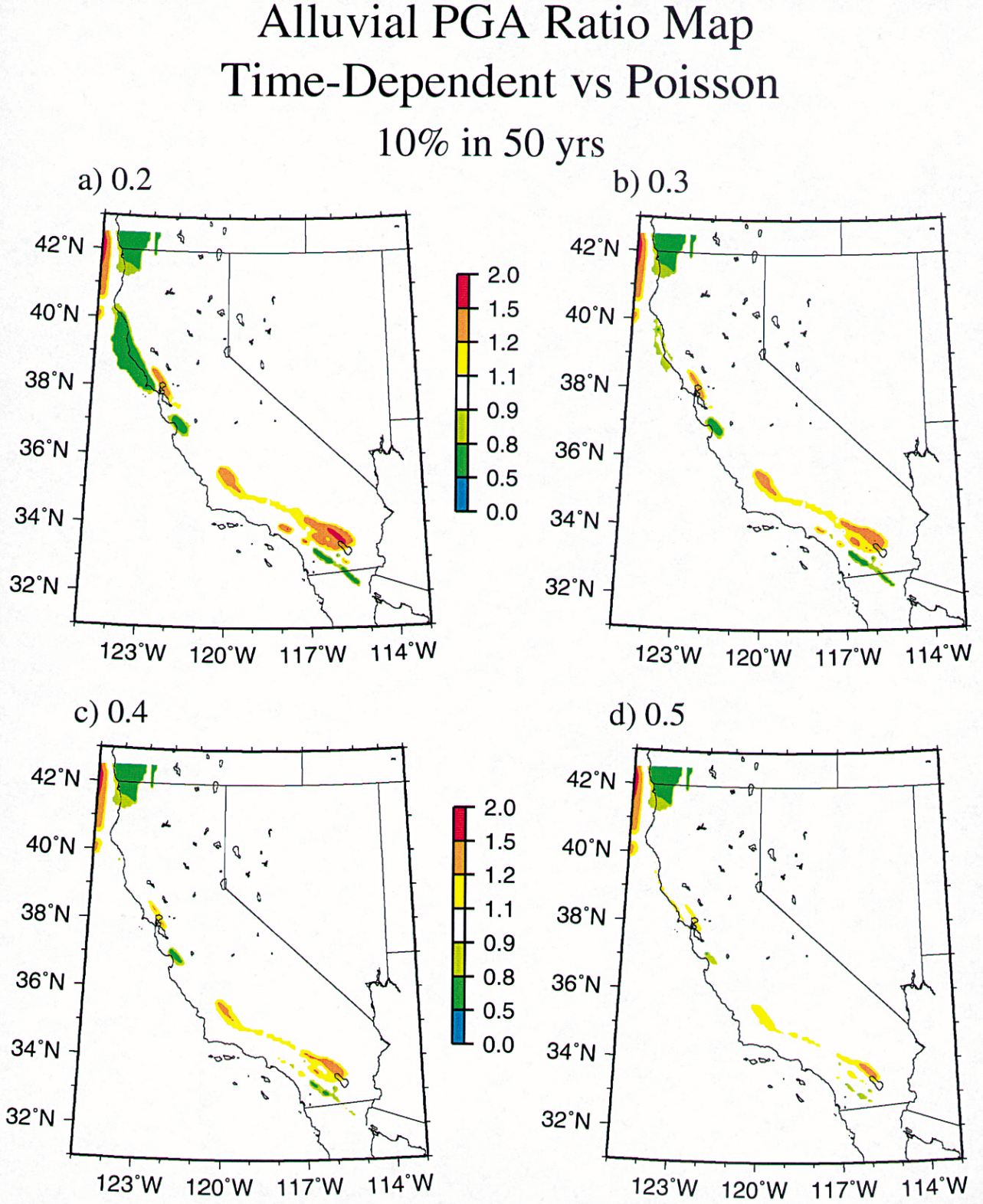

Figure 7. Same as Figure 6 except for a 10% exceedence in 50-year hazard.

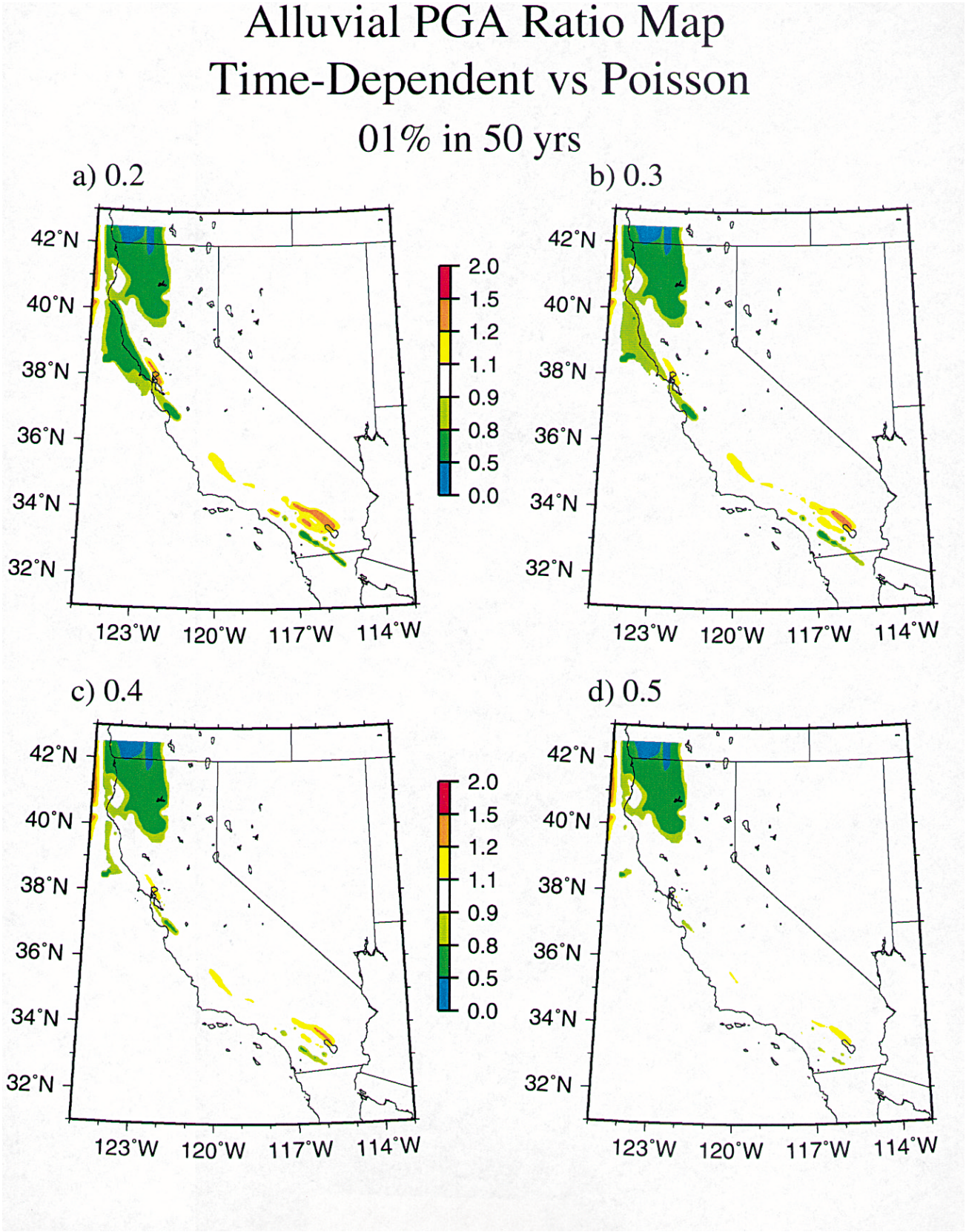

Figure 8. Same as Figure 6 except for a 1% exceedence in 50-year hazard.

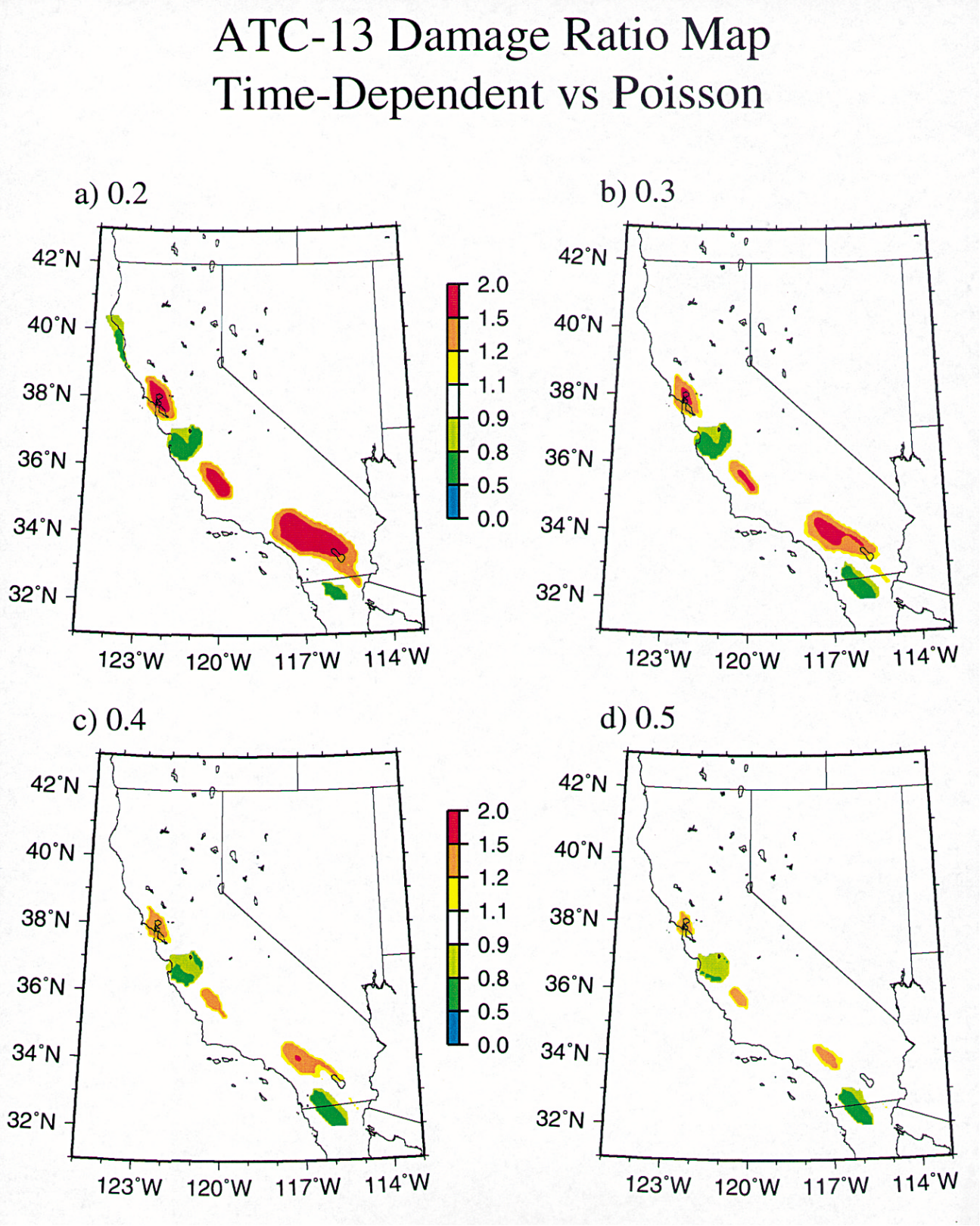

Figure 9. Maps of ratios of expected damage estimates from alluvial PGA hazard curves between time-dependent and Poisson models using the same cascading along the San Andreas fault system (see text). The presentation is as in Figure 6.

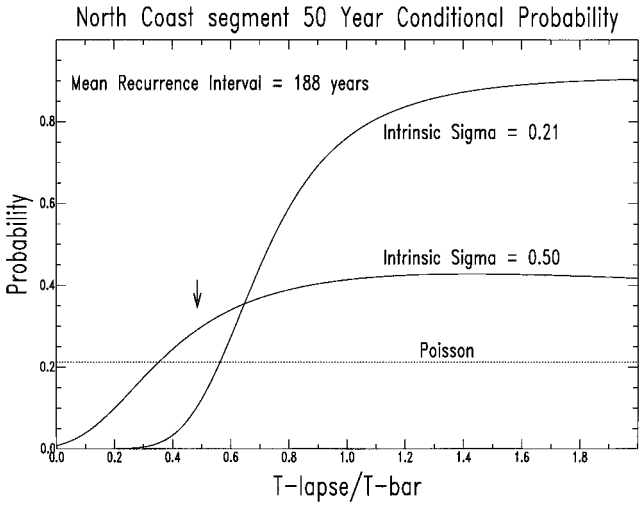

Figure 10. Comparison of 50-year conditional and Poisson probabilities for the North Coast Segment of the San Andreas fault. Conditional probabilities as a function of lapse time since the last characteristic earthquake (*T*-lapse) are plotted for intrinsic sigmas of 0.21 and 0.50. The lapse time is shown as a ratio of the mean-recurrence interval (*T*-bar). The arrow indicates the 1997 lapse time for this segment.

comes 69% larger than the CDMG Poisson model (Table 4). As shown in Figures 6a–9a, this results in PGA hazard and expected damage estimate ratios exceeding 20% along portions of the San Andreas fault. The degree of cascading for these three PSH models is the same and does not influence the difference in moment-rate budget for these cases.

When the CDMG Poisson model of Petersen *et al.* is compared with a noncascade version of that model (Table 4), the noncascade version has a 37% lower moment rate. Yet changes in PGA hazard and expected-damage estimates along the San Andreas fault between these two PSH models generally are less than 20% as shown in Figure 12. Only the 1% exceedence in 50 years PGA hazard changes (Figure 12c) exceed 20% along the San Andreas fault (except at Parkfield for 65% exceedence in 50 years).

The San Andreas fault cascade model is dominated by the magnitude assigned to the 1857 and 1906 ruptures. Petersen *et al.* (1996) originally assigned the historical magnitudes of 7.8 and 7.9 to the 1857 and 1906 ruptures included in the model. But using the fault area vs. magnitude relation of Wells and Coppersmith (1994) yields magnitudes of 7.7 and 7.8, respectively. Using the magnitudes derived from the Wells and Coppersmith fault area relation in the CDMG Poisson cascades model results in a Type A fault moment-rate budget about halfway between the standard CDMG Poisson cascade model and its noncascade version (Table 4).

When full cascade and noncascade versions of the $\sigma_i = 0.50$ time-dependent PSH model are compared with the CDMG Poisson PSH model, the Type A fault short-term moment-rate budget for the no cascade time-dependent version is 3% less than the Poisson model and the full cascade time-dependent version is 44% larger (Table 4). Additionally, when full cascade is compared to a noncascade version of a time-dependent model with the same intrinsic sigma, the Type A fault short-term moment-rate budget for the full-cascade model ranges from 29 to 48% higher than the Type A fault short-term moment-rate budget for the noncascade model, depending on the value of σ_i used. These larger differences (>40%) in short-term moment-rate budgets have large colored areas in Figures 3 and 4 (ratios exceeding 10%) for PGA hazard at 0.0021 and 0.0002 probability of occurrence (475 and 4975 year return periods), but smaller colored areas in Figures 2 and 5 for PGA hazard at 0.0210 probability of occurrence (63-year return period) and for expected-damage estimates.

A Monte Carlo sampling of the model uncertainty was run for the $\sigma_i = 0.50$ time-dependent PSH model with the cascading used by Petersen *et al.* (1996). The approach was that used by Cramer *et al.* (1996). The resulting mean and coefficient of variation (the standard deviation divided by the mean) for the short-term moment-rate distribution is 0.484×10^{19} N m/yr and 0.91. (Similar results were obtained for the CDMG/USGS Poisson PSH model of Petersen *et al.,* 1996.) As was found by Cramer *et al.* (1996), the largest contributors to this parametric uncertainty in moment rates are (1) the variation in maximum magnitude from the uncertainty in the Wells and Coppersmith (1994) magnitude vs. fault-area relation, and (2) the uncertainty in the fault-slip rate and characteristic earthquake-displacement observations. Thus the variations from the CDMG Poisson model in Table 4 (<70%) and between full and noncascade versions of the same PSH model in Table 4 (30–50%), are within the coefficient of variation of 91% for time-dependent modeling.

Conclusions

CDMG has assembled a time-dependent version of its PSH model for California for the purpose of sensitivity testing and highlighting components of the time-dependent models that do not have consensus within the earth-science community. For the most part, the time-dependent elements of the model are based on published consensus information. There are some nonconsensus aspects in the model: (1) the value of intrinsic sigma for all of California, (2) the amount of cascading of fault segments into larger earthquakes, (3) the choice of fault segments exhibiting time-dependence (i.e., the Parkfield segment, the Cholame segment, the Imperial fault, and Laguna Salada fault which the WGCEP94 treated as Poisson), and (4) the choice of the distribution used to model characteristic earthquake-recurrence intervals (i.e., log-normal instead of Brownian Passage Time, Weibull, or Gamma). For the latest consensus-mean value for intrinsic sigma of 0.50, the amount of cascading and the use of time-dependence results in few areas in which differences in PGA estimates exceeds 20% at a 0.0021 probability of

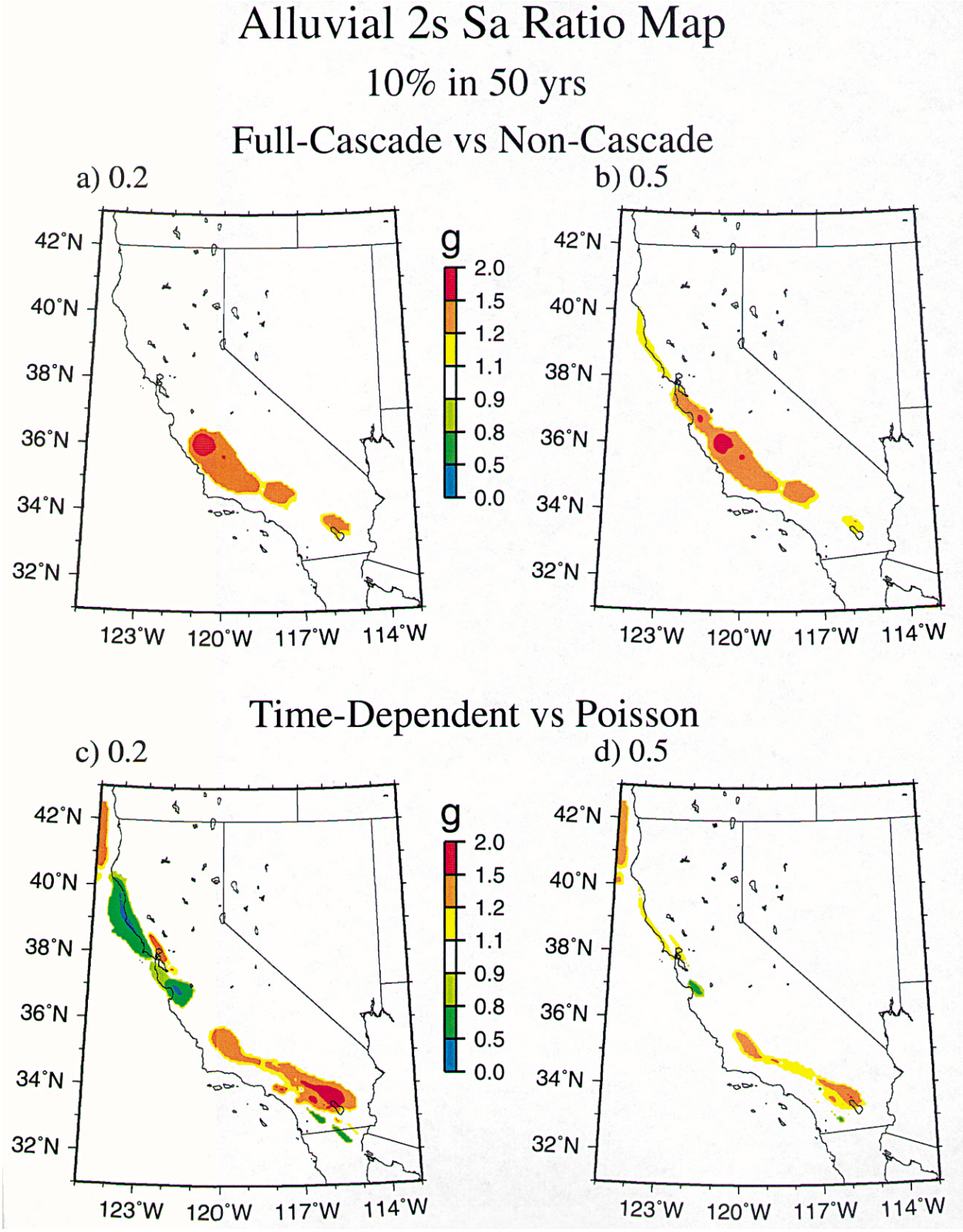

Figure 11. Maps of ratios of alluvial 2.0 sec spectral acceleration (*Sa*) for 10% exceedence in 50-year hazard: (a) full cascade over noncascade for 0.20 intrinsic sigma, (b) full cascade over noncascade for 0.50 intrinsic sigma, (c) time-dependent over Poisson for 0.20 intrinsic sigma, and (d) time-dependent over Poisson for 0.50 intrinsic sigma.

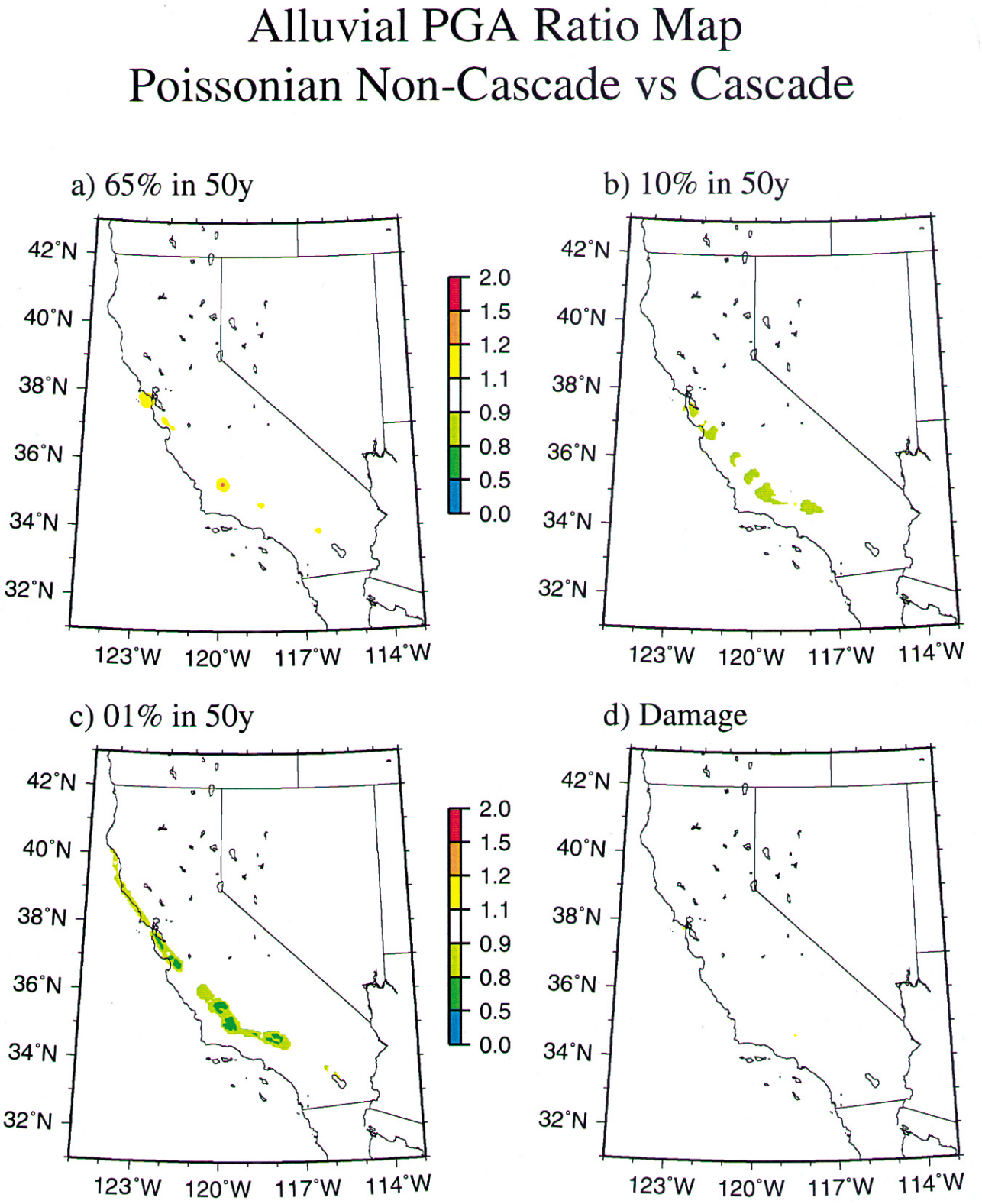

Figure 12. Maps of ratios of alluvial PGA hazard and expected damage estimates from alluvial PGA hazard curves between the CDMG Poisson model without cascading and with cascading (see text for cascading definitions). Ratio maps presented (noncascades over cascades) are for (a) 65% exceedence in 50-year hazard, (b) 10% exceedence in 50-year hazard, (c) 1% exceedence in 50-year hazard, and (d) expected-damage estimates.

Table 4
Annual Moment Rates from Type A Faults for Selected Sensitivity Test PSH Models for California (excluding the Cascadia subduction zone)*

Model	Annual Moment Rate (N m/yr)
Standard Models	
CDMG Poisson (Petersen et al., 1996)	0.105×10^{20}
Time-dependent, $\sigma_i = 0.50$ (this article)	0.148×10^{20}
Comparison Models (see text)	
Time-dependent, $\sigma_i = 0.20$	0.177×10^{20}
Poisson, No Cascade	0.066×10^{20}
Poisson, Cascade w/ 1857 & 1906 earthquake magnitudes reduced by 0.1 magnitude unit	0.086×10^{20}
Selected Sensitivity Test Models	
Time-dependent, full cascade, $\sigma_i = 0.50$	0.151×10^{20}
Time-dependent, no cascade, $\sigma_i = 0.50$	0.102×10^{20}
Time-dependent, full cascade, $\sigma_i = 0.20$	0.180×10^{20}
Time-dependent, no cascade, $\sigma_i = 0.20$	0.140×10^{20}

The annual moment rate for the remaining portion of the models (which is Poisson and hence fixed) is 0.121×10^{20} N m/yr (again excluding the Cascadia, subduction zone). Short-term annual-moment rates for time-dependent models are based on calculated 50-year conditional probabilities.

occurrence (475-year-return period or 10% exceedence in 50 years) or less. This is similar to the results of WGCEP94 (1995). Similarly, areas are small where expected damage estimates exceed changes of 20% when the difference exceeds $0.50 per thousand dollars of structure value. Hence the $\sigma_i = 0.50$ time-dependent PSH model produces similar PGA hazard and expected-damage estimates as the CDMG Poisson PSH model (see Figures 6d–9d). However this is not true for long period ground motions exceeding 1.0 second (see Figure 11).

Sensitivity tests on PGA hazard, expected-damage estimates, and PSH model moment-rate budgets show the impact of intrinsic sigma, full cascading vs. noncascading, and time-dependence vs. time-independence:

- Changes in PGA hazard and expected-damage estimates between time-dependent and time-independent models increase with decreasing intrinsic sigma.
- Changes in PGA hazard and expected-damage estimates between full cascading and not cascading (extremes) are insensitive to intrinsic sigma.
- Differences in PGA-hazard increase with increasing return period (decreasing probability of occurrence) although ratios may not always increase.
- Changes among short-term moment-rate budgets increase with decreasing intrinsic sigma and with the degree of cascading but are within the expected uncertainty in PSH time-dependent (and Poisson) modeling and have a small effect on PGA hazard and expected-damage estimates.

For expected damage and 10% in 50-year PGA hazard, changes between time-dependence and time-independence can exceed 20% within 20 km of the Type A faults for intrinsic sigmas of 0.2 to 0.3, similar to the results of Litehiser *et al.* (1992). Changes in expected-damage estimates due to cascading rarely exceed 10%, and changes in 10% in 50-year PGA hazard due to cascading generally do not exceed 20%. These results for expected damage are only for the Cao *et al.* (1999) approach to calculating expected damage by converting PGA to MMI and may not hold for expected damage calculated in another manner, such as directly from spectral acceleration and PGA.

Acknowledgments

The authors acknowledge and thank Norm Abrahamson and Ken Campbell for insightful reviews and comments. Their suggestions greatly improved the content of this article and are much appreciated.

References

Applied Technology Council (1985). ATC-13: earthquake damage evaluation data for California, Applied Technology Council, Redwood City, California, 492 pp.

Bakun, W. H., and T. V. McEvilly (1984). Recurrence models and Parkfield, California, earthquakes, *J. Geophys. Res.* **89,** 3051–3058.

Benjamin, J. R., and C. A. Cornell (1970). Probability, Statistics, and Decision for Civil Engineers, McGraw-Hill Publishing Company, New York, 684 pp.

Cao, T., M. D. Petersen, C. H. Cramer, T. R. Toppozada, M. R. Reichle, and J. D. Davis (1999). The calculation of expected loss from probabilistic seismic hazard, *Bull. Seism. Soc. Am.* **89,** 867–876.

Cramer, C. H., M. D. Petersen, and M. S. Reichle (1996). A Monte Carlo approach in estimating uncertainty for a seismic hazard assessment of Los Angeles, Ventura, and Orange counties, California, *Bull. Seism. Soc. Am.* **86,** 1681–1691.

Ellsworth, W. L., M. V. Matthews, R. M. Nadeau, S. P. Nishenko, P. A. Reasenberg, and R. W. Simpson (1999). A physically-based earthquake recurrence model for estimation of long-term earthquake probabilities, in *Proceedings of the Second Joint Meeting of the U.S.-Japan Natural Resources Panel on Earthquake Research,* Kobe, Japan, November 3–6, 1998, Geographical Survey Institute, Ministry of Construction (in press).

Frankel, A., C. Mueller, T. Barnhard, D. Perkins, E. V. Leyendecker, N. Dickman, S. Hanson, and M. Hopper (1996). National seismic hazard maps, June 1996 documentation *U. S. Geol. Surv. Open-File Report* 96-532.

Jacoby, G. C., D. E. Bunker, and B. E. Benson (1997). Tree-ring evidence for an A.D. 1700 Cascadia earthquake in Washington and northern Oregon, *Geology* **25,** 999–1002.

Litehiser, J., J. Marrone, and N. Abrahamson (1992). A preliminary model of firm foundation acceleration hazard in the San Francisco Bay area, *Earthquake Spectra* **8,** 225–257.

Nishenko, S. P., and R. Buland (1987). A generic recurrence interval distribution for earthquake forecasting, *Bull. Seism. Soc. Am.* **77,** 1382–1399.

Petersen, M. D., W. A. Bryant, C. H. Cramer, T. Cao, M. S. Reichle, A. D. Frankel, J. J. Lienkaemper, P. A. McCrory, and D. P. Schwartz (1996). Probabilistic seismic hazard assessment for the state of California, California Dept. of Conservation, Division of Mines and Geology, *Open-File Report 96-08,* 68 pp.

Petersen, M. D., C. H. Cramer, and M. S. Reichle (1997). Earthquakes that contribute to hazard and risk within the state of California (abstract), *EOS Trans. Am. Geophys. Union* **78,** F496.

Satake, K., K. Shimazaki, Y. Tsuji, and K. Ueda (1996). Time and size of a giant earthquake in Cascadia inferred from Japanese tsunami records of January 1700, *Nature* **379,** 246–249.

Savage, J. C. (1991). Criticism of some forecasts of the National Earthquake Prediction Evaluation Council, *Bull. Seism. Soc. Am.* **81,** 862–881.

Savage, J. C. (1992). The uncertainty in earthquake conditional probabilities, *Geophys. Res. Lett.* **19,** 709–712.

Sieh, K., M. Stuiver, D. Brillinger (1989). A more precise chronology of earthquakes produced by the San Andreas fault in southern California, *J. Geophys. Res.* **94,** 603–623.

Thatcher, W., G. Marshall, and M. Lisowski (1997). Resolution of fault slip along the 470-km-long rupture of the great 1906 San Francisco earthquake and its implications, *J. Geophys. Res.* **102,** 5353–5367.

Toppozada, T. R., and G. Borchardt (1998). Re-evaluation of the 1936 "Hayward" and the 1838 San Andreas fault earthquakes, *Bull. Seism. Soc. Am.* **88,** 140–159.

Toppozada, T. R., G. Borchardt, W. Haydon, M. Petersen, R. Olson, H. Lagoria, and T. Anvik (1995). Planning scenario in Humboldt and Del Norte counties, California for a great earthquake on the Cascadia subduction zone, California Dept. of Conservation, Division of Mines and Geology, Special Publication 115, 162 pp.

Trifunac, M. D., and A. G. Brady (1975). On the correlation of seismic intensity scales with the peaks of recorded strong ground motion, *Bull. Seism. Soc. Am.* **65,** 139–163.

Valentine, D., G. Vick, G. Carver, C. S. Manhart (1992). Late Holocene stratigraphy and paleoseismicity, Humboldt Bay, California, in Pacific Cell, Friends of the Pleistocene, Guidebook for the Field Trip to Northern Coastal California, A look at the southern end of the Cascadia Subduction Zone and The Mendocino Triple Junction, June 5–June 7, 1992, Friends of the Pleistocene, 182–187.

Wells, D. L., and K. J. Coppersmith (1994). New empirical relationships among magnitude, rupture length, rupture width, rupture area, and surface displacement, *Bull. Seism. Soc. Am.* **84,** 974–1002.

WGCEP88 (1988). Probabilities of large earthquakes occurring in California on the San Andreas fault, *U.S. Geol. Surv. Open-File Rept.* 88-398.

WGCEP90 (1990). Probabilities of large earthquakes in the San Francisco Bay region, California, *U.S. Geol. Surv. Circ. 1053.*

WGCEP94 (1995). Seismic hazards in southern California: probable earthquakes, 1994 to 2024, *Bull. Seism. Soc. Am.* **85,** 379–439.

WGNCEP96 (1996). Database of potential sources for earthquakes larger than magnitude 6 in northern California, *U.S. Geol. Surv. Open-File Rept. 96-705.*

Wu, S.-C., C. A. Cornell, and S. R. Winterstein (1995). A hybrid recurrence model and its implication on seismic hazard results, *Bull. Seism. Soc. Am.* **85,** 1–16.

California Dept. of Conservation
Division of Mines and Geology
801 K Street, MS 12-31
Sacramento, California 95814-3531

Manuscript received 16 June 1998.